Journal of Nanophotonics

Nanophotonics.SPIEDigitalLibrary.org

Investigation of defectiveness of multiwalled carbon nanotubes produced with Fe–Co catalysts of different composition

Sofya N. Bokova-Sirosh
Vladimir L. Kuznetsov
Anatoly I. Romanenko
Mariya A. Kazakova
Dmitry V. Krasnikov
Evgeniy N. Tkachev
Yury I. Yuzyuk
Elena D. Obraztsova

SPIE.

Investigation of defectiveness of multiwalled carbon nanotubes produced with Fe–Co catalysts of different composition

Sofya N. Bokova-Sirosh,[a,b,*] Vladimir L. Kuznetsov,[c,d,f] Anatoly I. Romanenko,[e,f] Mariya A. Kazakova,[c,d] Dmitry V. Krasnikov,[c,d] Evgeniy N. Tkachev,[e] Yury I. Yuzyuk,[g] and Elena D. Obraztsova[a,b]

[a]A. M. Prokhorov General Physics Institute RAS, 38 Vavilov Street, Moscow 119991, Russia
[b]National Research Nuclear University MEPhI, Kashirskoe shosse, 31, Moscow 115409, Russia
[c]Boreskov Institute of Catalysis SB RAS, Lavrentieva Avenue 5, Novosibirsk 630090, Russia
[d]Novosibirsk State University, Pirogova Avenue 2, Novosibirsk 630090, Russia
[e]Nikolaev Institute of Inorganic Chemistry, SB RAS, Lavrentieva Avenue 3, Novosibirsk 630090, Russia
[f]National Tomsk State University, 36, Lenina Avenue, Tomsk 634050, Russia
[g]Southern Federal University, Faculty of Physics, 5 Zorge Street, Rostov-on-Don 344090, Russia

Abstract. We have performed a study of CVD multiwalled carbon nanotubes (MWCNTs) produced with Fe–Co catalysts with a variable ratio of active metals. The Raman data were considered in combination with the temperature dependence of MWCNT conductivity. The data analysis is based on the point that the value of I_{2D}/I_D ratio correlates with the graphene fragment size. The fragments are considered as building blocks of MWCNTs. We showed that MWCNT defectiveness depends on the ratio of bimetallic active components in the Fe–Co catalyst. Thus, the ratio of I_{2D}/I_D increases and the D-mode intensity decreases while the Fe content in the catalyst increases. This also points to the reduction of defect number in the bigger graphene fragments. These results correlate with the data on conductivity temperature dependence. Namely, the increase of Fe content in the active component of the Fe–Co catalyst results in the increase of charge carrier concentration, which, in turn, indicates a decrease in MWCNT defectiveness. [DOI: 10.1117/1.JNP.10.012526]

Keywords: multiwalled carbon nanotubes; Raman spectroscopy; temperature dependence of conductivity; Fe–Co catalysts with variable ratio of active metals.

Paper 15136SS received Oct. 15, 2015; accepted for publication Feb. 11, 2016; published online Mar. 7, 2016.

1 Introduction

Multiwalled carbon nanotubes (MWCNTs) represent one of the promising materials in fast developing nanotechnology. At present, they have been used in a great number of applications.[1–4] The effectiveness of MWCNTs in composite materials depends on their structural parameters (diameter, number of walls, aspect ratio) and defectiveness. The latter is related to the presence of different types of defects like misalignment of the walls, disruptions, poorly graphitized layers, vacancies, Stone–Wales defects, and dislocations. This provides a possibility to consider curved graphene fragments as building blocks for carbon nanotubes. Thereby, the size of graphene fragments may be considered as one of the most important characteristics of the structural disorder in MWCNTs.

*Address all correspondence to: S. N. Bokova-Sirosh, E-mail: bokova.sirosh@gmail.com

1934-2608/2016/$25.00 © 2016 SPIE

High resolution transmission electron microscopy (HRTEM), scanning tunneling microscopy, and Raman spectroscopy can be used for direct studies of nanotube defects. The studies of MWNCT properties influenced by changes in graphitic structure provide indirect data on defects. In the previous papers, we showed a high sensitivity of Raman spectroscopy for estimation of the defective structure of MWCNTs and graphene flakes deposited on the nanotube surface.[5,6]

This analysis requires a consideration of behavior of D (disorder-induced), G (tangential mode), and 2D (two-phonon scattering) bands. The study of temperature dependence of electrical conductivity [$\sigma(T)$] and magnetic field dependences [$\sigma(B)$] of MWCNTs are also related to the nanotube diameter (in fact, the conductivity mechanism and electrophysical parameters of MWCNTs [electron coherent length (L_T), concentration of current carriers] depend on MWCNT defectiveness). The estimation of in-plane graphene fragment size (L_a) of MWCNTs via I_G/I_D ratio value correlates with the electron coherent length (L_T) calculated on the base of magnetoconductivity data for these samples. The I_{2D}/I_D ratio demonstrates almost linear dependence on the diameter of MWCNTs. We observed such behavior of the I_{2D}/I_D ratio for two sets of nanotubes produced with two different types of catalysts (Fe_2Co/Al_2O_3 and Co–Mn/Mg–Al with the fixed ratio of active metals).[6] It should be mentioned that each type of catalyst provides the linear dependence with its own specific slope. This implies that the nature of the active catalytic center affects the structure of nanotubes synthesized. It can be explained by the differences in kinetics and energy parameters of the main steps of MWCNT growth, namely (1) a decomposition of ethylene on the active metal particle with the formation of carbon atoms and hydrogen evolution; (2) a carbon atom diffusion (bulk and/or surface) to the interface of active metal particle with the growing nanotube; and (3) a carbon atom insertion into a metal–carbon bond in the interface of metal particle and nanotube. Despite the similarities of reaction mechanism of MWCNT synthesis with a metal catalyst, the differences in their specific energetic parameters are significant (an energy of M–C bonds, a carbon diffusion coefficient D, and so on). As a result, each type of catalyst component provides the formation of specific carbon deposits with the characteristic size of graphene flakes. As a consequence, MWCNTs synthesized in different processes with a variety of catalysts are characterized by a significant variation of structure and quality.

We have also proposed that the walls of MWCNTs may consist of the multidirectional graphene flakes packed into a mosaic structure. This conclusion was done on the base of analysis of conductivity measurements, Raman spectra, and mechanical properties of MWCNTs of different diameters.[6] Therefore, these defects should be considered along with the traditionally marked defects such as a misalignment of the walls, disruptions, poorly graphitized layers, and vacancies. The data obtained in our Raman experiments confirm the size variation of graphene flakes incorporated in any defect structures. Moreover, a high-temperature annealing of MWCNTs at 2400 to 3000 K results in the elimination of structural defects of nanotube walls.[7] In other words, it leads to an increase of the graphene building block size. This statement was proved by a dramatic increase of I_{2D}/I_D ratio (up to 10 times) after annealing and by the temperature dependences of electrical conductivity and TEM images.[5]

In the present paper, we have studied properties of MWCNTs produced with the Fe–Co catalysts containing a variable Fe:Co ratio. The Raman spectroscopy and measurements of the temperature dependence of conductivity, revealing the features associated with changes in MWCNT structure, were applied for measurement depending on the ratio of active metals to catalyst.

2 Experimental Procedure

MWCNTs were grown using catalysts with a variable composition of active Fe–Co alloy.[8] Catalysts $Fe-Co/Al_2O_3$ were prepared with the Pechini method.[9] It is based on the preliminary distribution of metal ions (Fe, Co, Al) in a three-dimensional polymeric matrix. The annealing of this matrix afterwards leads to the appearance of a system of mixed spinel-like oxides.[10] Different Co content in the Fe–Co alloy was used (0, 22, 25, 29, 33, 50, 60, 67, 71, 100 at. %) during the synthesis of catalysts. MWCNT synthesis was carried out in a quartz tubular reactor at 670°C in Ar/C_2H_4 flow (400 sccm; 1:1; 15 min). The average diameter of

MWCNTs was affected by the composition of the active Fe–Co alloy. MWCNT diameter distribution was monitored by TEM (JEM-2010). For each sample the diameter distribution was estimated using 300–600 MWCNT images obtained by TEM at magnifications of ×50,000 and ×400,000.

The Raman spectroscopic analysis of multiwalled nanotube (MWNT) powders has been performed with a Renishaw's inVia Reflex spectrometer in microscopic configuration with the spectral resolution of 2 cm^{-1}. The radiation of Ar laser with the wavelength of 514.5 nm was used for spectra excitation. The Raman spectra of MWNTs have been recorded in three spectral regions: D (disorder-induced), G (graphite), and 2D (two-phonon scattering) bands. All spectra were normalized with respect to D-mode.

The electrical contacts were made by 0.1 mm silver wires. The temperature dependences of conductivity $\sigma(T)$ of MWNTs produced with different types of catalysts were measured by a four point-probe technique in the temperature range 4.2 to 300 K. For electrical measurements the MWNT powder was pressed in a glass cylinder. Our previous studies of powder carbon nanostructures carried out by this method[11–16] showed a stability and reproducibility of conductivity measurement results.

3 Results and Discussion

3.1 *Defective Structure of Multiwalled Carbon Nanotubes*

Such structural and topological defects of MWCNTs as the planar fragments, Y-junctions, and terminated and curved walls can be observed by HRTEM (Fig. 1). The latter can be referred to the presence of penta- and heptagon units in the "hexagonic" structure of sp^2-carbon. Nevertheless, it is not possible to distinguish between the presence of sp^3-bonded carbon or the missing atoms in the lattice using HRTEM. Moreover, this method does not provide quantitative information of the defective structure of nanotubes.

However, the abovementioned defects imply the presence of ideal structure islands within the nanotube wall. Previously, we have shown the interconnection of these islands via the grain boundary mechanism (Fig. 2). In the case of the sp^2-carbon structure the grain boundaries implement through the penta- and heptagon sequences on the boundaries between the ideal structure islands.[17]

The "graphene-building block" structure of nanotube walls can be indirectly observed by x-ray diffraction with synchrotron radiation (XRD patterns not presented here). While a coherence length of C (002) reflex can be considered as the thickness of nanotube walls, the coherence

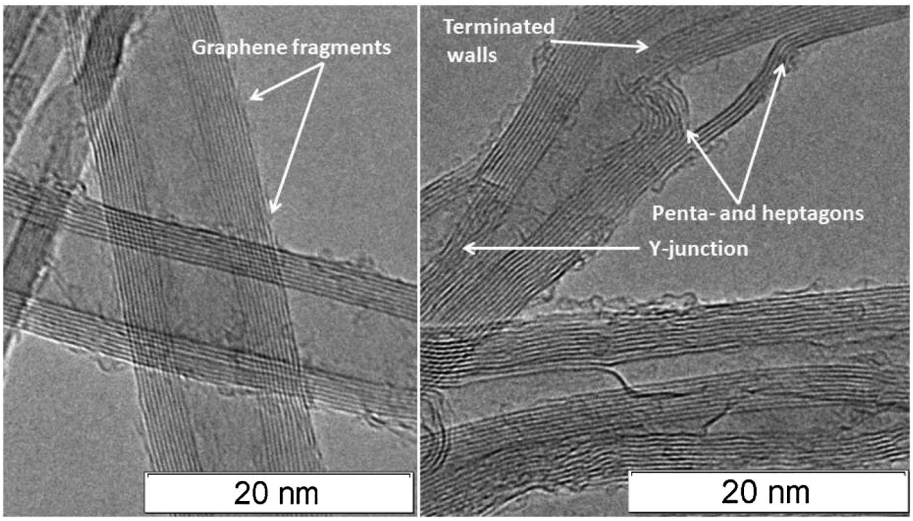

Fig. 1 HRTEM image of MWCNTs produced with Fe_2Co catalyst. The presence of some defects in MWCNT structure is shown.

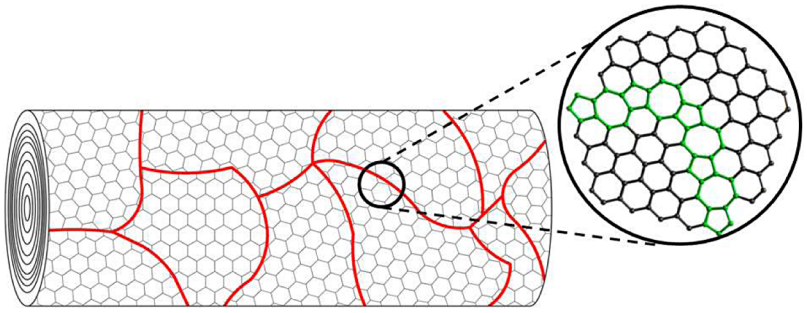

Fig. 2 The scheme of the nanotube wall consisted of graphene building blocks connected via a grain boundary mechanism. The border consisted of hepta- and pentagons as shown in the inset.

length of C (100) reflex can be referred to the size of nondefect sp^2-carbon in the plane of the nanotube walls. In other words, this can be considered as an effective size of the ideal graphene sheets within the nanotube. However, a turbostratic structure of MWCNTs prohibits a quantitative description of nanotube texture by XRD data. Nevertheless, it still provides only a qualitative information.

Thereby, only Raman spectroscopy can provide a bulk quantitative estimation of the defect concentration in the nanotube wall.

3.2 *Optical Studies*

The so-called "radial breathing modes" (RBM) are normally used for characterization of single-wall carbon nanotubes. The positions of these bands of low frequency are determined by the geometric parameters of nanotubes. The Raman features associated with RBM for MWCNTs usually have too small a shift to be observed. The Raman signal of small diameter inner tubes could be detected under the exact resonance excitation. We have observed no signal in the spectral range of RBM. Therefore, major attention has been paid to the D, G, and 2D bands in the Raman spectra. The presence of a D band with the frequency of 1350 cm^{-1} is related to a disorder-induced breaking of Raman selection rules for small graphene or graphite fragments, the presence of a G band (1580 cm^{-1}) corresponds to tangential modes of sp^2 carbon lattice, and a 2D band (2680 cm^{-1}) corresponds to two-phonon scattering. However, the intensity ratio of these modes was of greatest interest. We have already mentioned that the slope of I_{2D}/I_D dependence on the nanotube diameter reflects the difference in the nature of changes in the defect MWNTs produced using various types of catalysts.[6]

Figure 3 shows the Raman spectra of MWCNTs produced with Fe–Co catalysts with a variable ratio of active metals. The increase of Fe content results in the increase of intensity of 2D Raman lines, while there are almost no variations in the intensities of D and G. Figure 4 demonstrates the dependence of intensity ratio I_{2D}/I_D on the ratio of catalysts to active components.

Thus, an increase of Fe content in the active catalyst component leads to the growth of I_{2D}/I_D ratio, while the D-mode somewhat decreases with respect to the G-mode, indicating a decrease in the number of defects. These results correlate with the data obtained in the study of the temperature dependence of electrical conductivity. Namely, by increasing the Fe content in the catalyst, the density of states at Fermi level N (E_F) increases, indicating a shortage of defect number in MWCNTs (see below). Also, it should be noted that the ratio of intensities of considered Raman modes (D, G, and 2D) may vary within one sample. This indicates the heterogeneity of the material but does not change the overall trend.

Previously, we observed that I_{2D}/I_D ratio demonstrates almost linear dependence on the diameter of MWCNTs.[18] Thus, the dependence of the I_{2D}/I_D ratio on catalyst composition should be accounted not only for the chemical composition of active particles but also for MWCNT diameter. Figure 5 shows the comparison of two sets of Raman data: (1) the I_{2D}/I_D ratio versus a mean diameter of MWCNTs produced with the Fe–Co catalysts with a variable ratio of active metal (this paper) and (2) the I_{2D}/I_D ratio versus a mean diameter of MWCNTs produced with the Fe–Co catalysts with a fixed ratio of Fe and Co, equal to 2 (Fig 5, blue dashed line).[18] The diameter of MWCNTs produced with the catalysts with variable

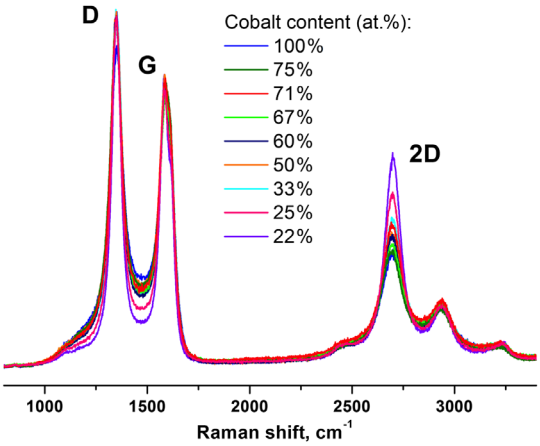

Fig. 3 The Raman spectra of MWNT synthesized on the basis of Fe–Co catalyst.

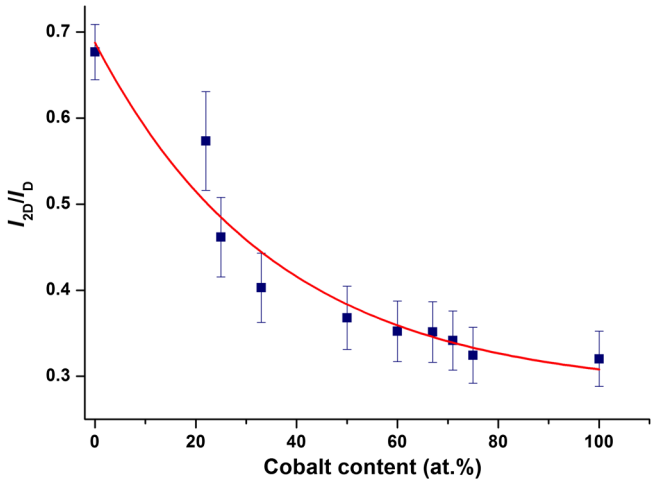

Fig. 4 The dependence of intensity ratio I_{2D}/I_D on the ratio of catalysts to active components (Fe/Co).

Fe and Co ratio (while the atomic concentration of the active metal was fixed) increases with growth of iron content. We obviously observe the deviation from the linearity of the I_{2D}/I_D ratio, being characteristic for the MWCNT set produced with the Fe–Co catalysts with a variable ratio of active metal (this paper). It can be explained in terms of differences in kinetics and energy parameters of the main steps of MWCNT growth characteristic for the element composition of active alloys. This statement also supports our previous results discussed in Ref. 6.

The Raman data allow us to estimate a typical size of graphene fragments using the value of the I_D/I_G ratio. Tuinstra and Koenig[19] presented the study showing the inverse proportionality of the ratio of D and G band intensities to the in-plane crystallite sizes L_a. Later, the influence of laser photon energy has been detected[20,21] and the general formula giving L_a of nanographite systems (for any excitation laser photon energy in the visible range) has been presented by Cançado et al.[22] For MWCNTs produced with the catalyst containing different ratios of Fe/Co, we have estimated $L_a(\mathrm{C}) \sim 14$ nm using their approach.[22]

3.3 *Electron Transport Properties*

The temperature dependences of conductivity $\sigma(T)$ of MWCNTs produced with different types of catalysts are shown in Fig. 6 in the temperature range of 4.2 to 300 K. For electrical measurements, the powder MWCNTs were pressed in a glass cylinder. Our previous researches of

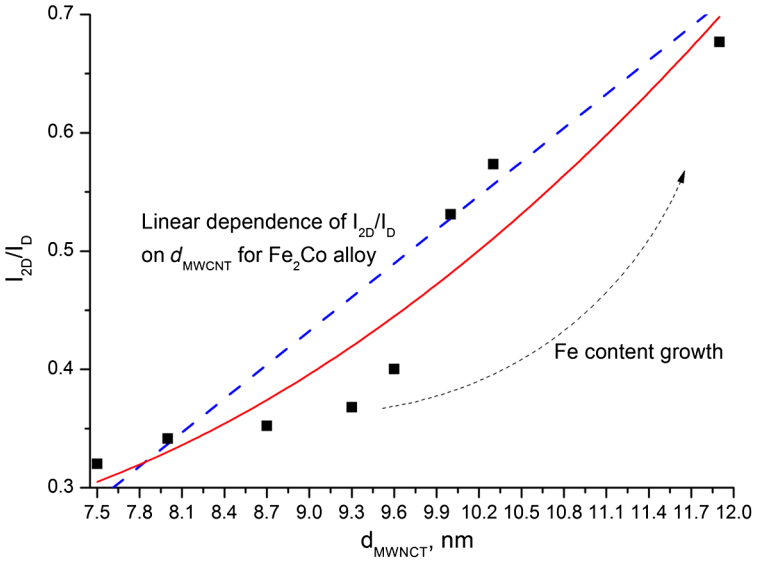

Fig. 5 The dependence of I_{2D}/I_D ratio on the mean diameter of MWCNTs produced with a Fe–Co catalyst with a variable Fe–Co ratio (red line). Fe content in the Fe–Co alloy grows along with the nanotube diameter. The blue dashed line represents the influence of the I_{2D}/I_D ratio on MWCNT mean diameters of active Fe_2Co catalyst particles.[18] The green dashed line corresponds to the dependence of diameter (with active pure Fe and pure Co catalyst particles) on the I_{2D}/I_D ratio.

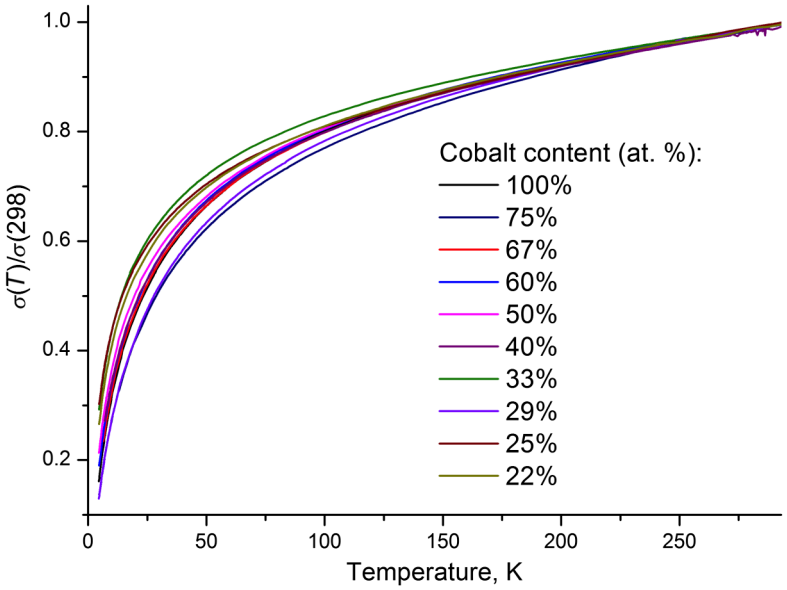

Fig. 6 The temperature dependences of conductivity $\sigma(T)$ of MWNTs produced with different types of catalysts.

powder carbon nanostructures carried out by this method showed the stability and reproducibility of such conductivity measurement results.

MWCNTs show a temperature dependence of conductivity as $\sigma(T) \sim \exp(-T^{-1/2})$ (Fig. 6), which can be described within the Coulomb blockade theory (Efros–Shklovskii variable range hopping model [ES] of conductivity) or within the quasi one-dimensional (1-D) variable range hopping conductivity (VRHC) (Mott low):

$$\sigma(T) = \sigma_0 \exp[(-T_0/T)^{1/2}], \tag{1}$$

where σ_0 is constant, $T_0 = C_{\mathrm{VRHC}}\alpha^{-1}/\mathrm{k_B}N(E_\mathrm{F})$, $C_{\mathrm{VRHC}} \approx 1$ for 1-D VRHC, $T_0 = T_{\mathrm{ES}} = C_{\mathrm{ES}}\alpha^{-3}/\mathrm{k_B}N(E_\mathrm{F})$, $C_{\mathrm{ES}} = (2.8/4\pi)$, α^{-1} is the length on which the amplitude of the wave function falls down ($\alpha^{-1} \approx 10$ Å), $N(E_\mathrm{F})$ is the density of localized states at the Fermi level E_F, and $\mathrm{k_B}$ is the Boltzmann constant. It is worthy of notice that for both mechanisms of dependence [Eq. (1)] (1-D WRHC or ES) the inversely proportional dependence of $N(E_\mathrm{F})$ on the parameter T_0 takes place. From $N(E_\mathrm{F})$ it is possible to estimate the current carrier concentration n from the ratio $n \sim 2/3\ N(E_\mathrm{F})/E_\mathrm{F}$.

As can be seen from Fig. 4, all curves are linear in co-ordinates $\ln(\sigma)$ versus $T^{-1/2}$ [co-ordinates of dependence (1)] at temperature $T < 70$ K.

Using the results of experimental data approximations (Fig. 7) from Eq. (1) we have determined the $N(E_\mathrm{F})$—the density of localized states at the Fermi level E_F for all samples. Using the ratio $N(E_\mathrm{F}) \sim 3/2 \cdot n \cdot E_\mathrm{F}$ ($E_\mathrm{F} \sim 0.1$ eV), we have also estimated the current carrier concentration n from the obtained $N(E_\mathrm{F})$ (Fig. 8).

Thus, an increase of Fe content in the catalyst results in the increase of concentration for current carriers, which, in turn, indicates a decrease of MWCNT defectiveness. These results correlate with the data obtained with the Raman spectroscopy. The ratio of I_{2D}/I_D increases and the D mode decreases with respect to the G mode when the Fe content in the catalyst increases, which also points to the reduction of defect number.

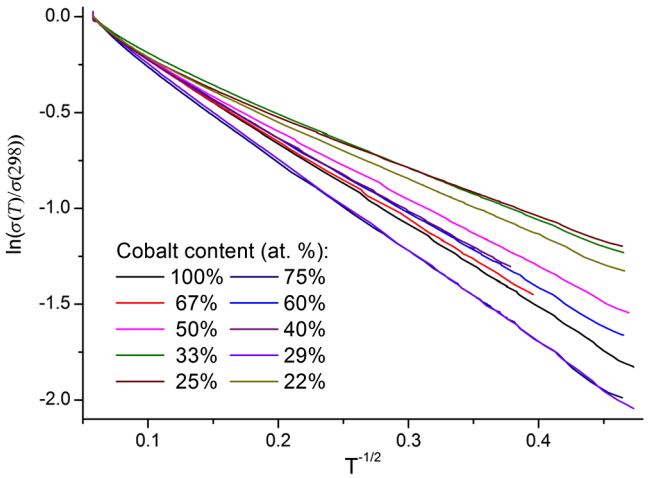

Fig. 7 The dependences of logarithm conductivity $\ln(\sigma)$ on $T^{-1/2}$ of MWNTs produced with different types of catalysts. The straight line shows the approximation of experimental data by Eq. (1).

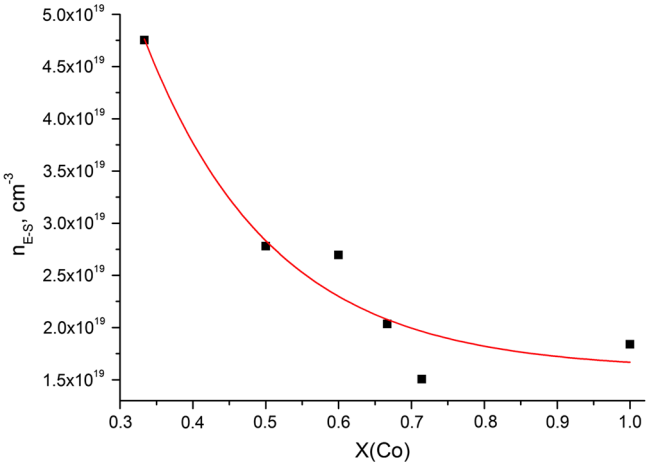

Fig. 8 The dependences of current carrier concentration for MWCNTs on the Co content in Fe–Co alloy active particles of MWCNT synthesis catalyst.

4 Conclusion

In this paper we show that MWCNT defectiveness is a function of Fe–Co catalyst composition. Thus, the increase of Fe content in the active component of the Fe–Co catalyst results in the increase of current carrier concentration. This, in turn, indicates a decrease of MWCNT defectiveness. These results correlate with the data obtained with Raman spectroscopy. The ratio of I_{2D}/I_D increases and the D mode decreases with respect to the G mode when the Fe content in the catalyst increases. This also points to the reduction of the number of defects (with the size of graphene fragment). The ratio of I_{2D}/I_D correlates with the size of graphene fragments.

Acknowledgments

The reported study was funded by the Russian Foundation for Basic Research via grants 15-32-70013 mol_a_mos (to S.N.B-S to conduct Raman spectroscopic studies) and 16-32-60046 mol_a_dk (to M.A.K. to obtain the catalyst samples), 14-32-50078 mol_rf, 15-32-50242 mol_rf_nr. Authors also would like to thank Dr. K.V. Elumeeva. A.V. Ischenko, and Dr. A. N. Shmakov for catalyst characterization, TEM, and XRD studies, respectively.

References

1. M. S. Dresselhaus et al., "Electronic, thermal and mechanical properties of carbon nanotubes," *Philos. Trans. R. Soc. Math. Phys. Eng. Sci.* **362**, 2065–2098 (2004).
2. M. S. Dresselhaus, A. Jorio, and R. Saito, "Characterizing graphene, graphite, and carbon nanotubes by Raman spectroscopy," *Annu. Rev. Condens. Matter Phys.* **1**, 89–108 (2010).
3. S. Yamashita, Y. Saito, and J. H. Choi, Eds., *Carbon Nanotubes and Graphene for Photonic Applications*, Woodhead Publishing Limited, Oxford, Cambridge, Philadelphia, New Delhi (2013).
4. M. F. L. De Volder et al., "Carbon nanotubes: present and future commercial applications," *Science* **339**, 535–539 (2013).
5. V. L. Kuznetsov et al., "Multi-walled carbon nanotubes with ppm level of impurities," *Phys. Status Solidi B* **247**(11–12), 2695–2699 (2010).
6. V.L. Kuznetsov et al., "Raman spectra for characterization of defective CVD multi-walled carbon nanotubes," *Phys. Status Solidi B* **251**(12), 2444–2450 (2014).
7. K. V. Elumeeva et al., "Reinforcement of CVD grown multi-walled carbon nanotubes by high temperature annealing," *AIP Adv.* **3**(11), 112101 (2013).
8. D. V. Krasnikov et al., "Investigation of Fe-Co catalyst active component during multi-walled carbon nanotube synthesis by means of synchrotron radiation x-ray diffraction," *Bull. RAS Phys.* **77**(2), 155–158 (2013).
9. M. Popa, J. Frantti, and M. Kakihana, "Lanthanum ferrite $LaFeO_3 + d$ nanopowders obtained by the polymerizable complex method," *Solid State Ion.* **154**, 437–445 (2002).
10. V. L. Kuznetsov et al., "In situ and ex situ time resolved study of multi-component Fe-Co oxide catalyst activation during MWNT synthesis," *Phys. Status Solidi B* **249**(12), 2390–2394 (2012).
11. V. L. Kuznetsov et al., "Electrical resistivity of graphitized ultra-disperse diamond and onion-like carbon," *Chem. Phys. Lett.* **336**, 397–404 (2001).
12. A. I. Romanenko et al., "Heterogeneous electronic states in carbon nanostructures with different dimensionalities and curvatures of the constituent graphene layers," *Phys. Usp.* **48**, 958–962 (2005).
13. A. I. Romanenko et al., "Influence of helium, hydrogen, oxygen, air and methane on conductivity of multiwalled carbon nanotubes," *Sens. Actuators, A* **138**, 350–354 (2007).
14. E. N. Tkachev et al., "Separating weak-localization and electron-electron-interaction contributions to the conductivity of carbon nanostructures," *J. Exp. Theor. Phys.* **105**(1), 223–226 (2007).
15. T. I. Buryakov et al., "Influence of curvature of graphene layers of multiwalled carbon nanostructures on electrophysical properties," *Int. J. Nanosci.* **8**, 19 (2009).

16. Z. R. Ismagilov et al., "Structure and electrical conductivity of nitrogen-doped carbon nanofibers," *Carbon* **47**, 1922–1929 (2009).
17. Z. Zhang et al., "Graphene: unraveling the sinuous grain boundaries in graphene," *Adv. Funct. Mater.* **25**(3), 496–496 (2015).
18. S. N. Bokova et al., "Raman diagnostics of multi-wall carbon nanotubes with a small wall number," *Phys. Status Solidi B* **247**, 2827–2830 (2010).
19. F. Tuinstra and J. L. Koenig, "Raman spectrum of graphite," *J. Chem. Phys.* **53**, 1126 (1970).
20. T. P. Mernagh, R. P. Cooney, and R. A. Johnson, "Raman spectra of graphon carbon black," *Carbon* **22**, 39–42 (1984).
21. D. S. Knight and W. White, "Characterization of diamond films by Raman spectroscopy," *J. Mater. Res.* **4**, 385 (1989).
22. L. G. Cançado et al., "General equation for the determination of the crystallite size LaLa of nanographite by Raman spectroscopy," *Appl. Phys. Lett.* **88**(16), 163106 (2006).

Sofya N. Bokova-Sirosh graduated from the Moscow Engineering Physics Institute in 2003 and received her PhD from the A.M. Prokhorov General Physics Institute (GPI RAS) in 2007. Currently, she is a senior researcher in GPI RAS. Her research interests are studies of the single and multiwall carbon nanotube-based materials with optical spectroscopy techniques (Raman scattering, optical absorption). The main results are presented in 58 publications, including 19 articles in peer-reviewed journals.

Vladimir L. Kuznetsov received his diploma degree in chemistry from Novosibirsk State University (NSU) in 1973, and his PhD from the Boreskov Institute of Catalysis in 1978. Currently, he is the head of a research group at the Boreskov Institute of Catalysis and a lector of catalysts at NSU. He is the author or coauthor of more than 200 articles in refereed journals, nearly 450 conference papers, 10 patents, and six book chapters.

Anatoly I. Romanenko received his diploma degree from NSU in 1973, his PhD from the Institute of Semiconductor Physics in 1986, and his doctor of science from the Institute of Inorganic Chemistry in 2000. Currently, he is the head of the Laboratory of Low Temperature Physics. He is the author of more than 100 articles in major refereed journals and nearly 200 conference papers.

Mariya A. Kazakova graduated from the Faculty of Natural Sciences of NSU in 2008 and received her PhD from Boreskov Institute of Catalysis SB RAS, in 2012. Her scientific interests mainly lie in the field of heterogeneous catalysis and carbon materials (particularly synthesis, testing, and fabrication of novel composite materials). She is the author or coauthor of 12 papers in peer-reviewed journals and nearly 40 conference papers.

Dmitry V. Krasnikov graduated from NSU, Novosibirsk, in 2012. He started his career at Boreskov Institute of Catalysis in 2008. Currently, he is a junior research scientist there. His scientific interests concern carbon nanomaterials, heterogeneous catalysis, and material science. He won the PhD student award of the European Catalysis Society two times (2013, 2015). He is the author or coauthor of 12 articles in refereed journals and 46 conference papers.

Evgeniy N. Tkachev received his MS degree from NSU in 2007, his PhD from the Institute of Inorganic Chemistry, Russian Academy of Sciences, in 2010. Currently, he is a senior research assistant at the Institute of Inorganic Chemistry. He is the coauthor of more than 25 articles in refereed journals. His research interests consist of electron transport of carbon materials and composites based on them, oxides of cobalt, and other nanoscale materials.

Yury I. Yuzyuk received his MS degree in physics in 1982 and his PhD in condensed matter physics in 1989, both from Rostov State University, Rostov-on-Don, Russia. He has 30 years of hands-on experience in Raman spectroscopy of molecular crystals, ferroelectric crystals, ceramics, thin films, superlattices, semiconductors, carbon nanotubes, and liquid crystals. He has coauthored more than 160 journal papers and three books. He has participated in a number of research projects and is coordinator of two French–Russian projects.

Elena D. Obraztsova graduated from the Physics Department of M.V. Lomonosov Moscow State University (MSU) in 1981. She received her PhD in optics at MSU in 1990. Since 1992, she has worked at A.M. Prokhorov General Physics Institute, RAS, heading the Nanomaterials Spectroscopy Laboratory since 2001. Her scientific interests concern optical spectroscopy of low-dimensional materials. She is a coauthor of more than 230 papers in reviewed journals. She was a supervisor of 10 PhD defended theses.